frontiers in Immunology

TYPE Original Research
PUBLISHED 13 November 2026
DOI 10.3389/fimmu.2026.1993392

Check for updates

OPEN ACCESS

EDITED BY
Zhiwen Luo,
Fudan University, China

REVIEWED BY
James J. Vanhie,
Scintica Instrumentation Inc, Canada
Forrest Lee Baker,
University of South Carolina, United States

*CORRESPONDENCE
Alejandro Lucia
alejandro.lucia@universidadeuropea.es
Carmen Fiuza-Luces
cfiuza.imas12@h12o.es

†These authors share first authorship

‡These authors share senior authorship

RECEIVED 09 September 2026
REVISED 21 October 2026
ACCEPTED 29 October 2026
PUBLISHED 13 November 2026

CITATION
Yanguas-Casás N, Neu MA, Plaza-Florido A, Ramos ESC, Yagüe-Peñuelas R, Garrido-Rodríguez E, Spreafico F, Zardo W, Gasparini P, Chisari M, Wiskemann J, Schwarzländer G, Dreismickenbecker E, Paret C, Wypyrsczyk L, Kuehn M, Lehmann N, Faber J, Lucia A and Fiuza-Luces C (2026) Exploratory immune signatures associated with exercise in pediatric solid tumors. *Front. Immunol.* 17:1993392. doi: 10.3389/fimmu.2026.1993392

COPYRIGHT
© 2026 Yanguas-Casás, Neu, Plaza-Florido, Ramos, Yagüe-Peñuelas, Garrido-Rodríguez, Spreafico, Zardo, Gasparini, Chisari, Wiskemann, Schwarzländer, Dreismickenbecker, Paret, Wypyrsczyk, Kuehn, Lehmann, Faber, Lucia and Fiuza-Luces. This is an open-access article distributed under the terms of the Creative Commons Attribution License (CC BY). The use, distribution or reproduction in other forums is permitted, provided the original author(s) and the copyright owner(s) are credited and that the original publication in this journal is cited, in accordance with accepted academic practice. No use, distribution or reproduction is permitted which does not comply with these terms.

Exploratory immune signatures associated with exercise in pediatric solid tumors

Natalia Yanguas-Casás[1†], Marie A. Neu[2,3†], Abel Plaza-Florido[4], Eva S.C. Ramos[5], Rodrigo Yagüe-Peñuelas[5], Eva Garrido-Rodríguez[1], Filippo Spreafico[6], William Zardo[7], Patrizia Gasparini[7], Marco Chisari[7], Joachim Wiskemann[8], Gabriele Schwarzländer[8], Elias Dreismickenbecker[2,3], Claudia Paret[2,3], Lena Wypyrsczyk[2,3], Mareike Kuehn[2,3], Nadine Lehmann[2,3], Joerg Faber[2,3], Alejandro Lucia[1,5*‡] and Carmen Fiuza-Luces[1*‡]

[1]Research Institute of Hospital 12 de Octubre ("imas12"), Madrid, Spain, [2]Pediatric Hematology/Oncology, Department of Pediatrics, University Medical Center of the Johannes Gutenberg-University Mainz, Mainz, Germany, [3]Childhood Cancer Center Mainz, University Cancer Center Mainz (UCT Mainz), University Medical Center of the Johannes Gutenberg-University Mainz, Mainz, Germany, [4]Research Center for Exercise Medicine and Sleep/Pediatric Exercise and Genomics Research Center, Department of Pediatrics, School of Medicine, University of California, Irvine, Irvine, CA, United States, [5]Department of Sports Sciences. Faculty of Medicine, Health and Sports. Universidad Europea de Madrid, Madrid, Spain, [6]Oncology Unit, IRCCS Istituto Giannina Gaslini, Genova, Italy, [7]Fondazione IRCCS Istituto Nazionale dei Tumori di Milano, Milano, Italy, [8]Department of Medical Oncology, Working Group Exercise Oncology, a partnership between DKFZ and University Medical Center Heidelberg, Heidelberg University Hospital and National Center for Tumor Diseases, Heidelberg, Germany

Background: Exercise has emerged as a promising supportive strategy in pediatric oncology; however, its immunological effects, particularly at the level of specific immune cell subsets, remain poorly understood.

Objective: We aimed to evaluate the effects of a structured exercise intervention on immune system-related outcomes in pediatric patients with solid tumors, with a particular focus on identifying potential exercise-associated immune signatures using high-dimensional profiling.

Methods: This immune-focused ancillary study included a subset of 29 participants enrolled in the parent multicenter randomized controlled FORTEe trial, where the intervention was an 8-10–week exercise program performed shortly after tumor diagnosis. Peripheral blood mononuclear cells were collected before and after the intervention period in 14 and 15 patients allocated to the exercise and control group, respectively. Spectral flow cytometry combined with unsupervised clustering was used to comprehensively characterize the relative distribution and phenotypic profile of circulating immune populations, including natural killer (NK) cells, T cell subsets, and dendritic-like populations. Intervention effects were evaluated using a two-way mixed ANOVA. The group-by-time interaction was considered the primary effect of interest. Given the exploratory nature of this ancillary analysis, both nominal and false-discovery-rate–adjusted p values were reported.

Results: The exercise intervention did not affect the relative distribution of major circulating immune cell populations or NK cell phenotypes ($p>0.05$). However, high-dimensional analysis identified 20 immune metaclusters (MC), among which three (MC-01, MC-02 and MC-04) showed significant nominal, but not adjusted,

group-by-time interactions. The relative abundance of MC-01 (+11.3%) and to a much lesser degree of MC-02 (+0.9%) increased in controls but both populations decreased in the exercise group (–2.0% and –3.1%, respectively) whereas the MC-04 population decreased in controls (–4.4%) while increasing with the exercise intervention (+5.0%). MC-01 comprised an antigen-presenting myeloid population displaying dendritic cell-like features (characterized by CD11b, CD11c, CD14, CD16, CD95, and CD141 expression), MC-02 corresponded to a mature $CD19^+$ $CD20^+$ $CD45RA^+$ $HLADR^+$ population, whereas MC-04 corresponded to a $CD8^+$ TEMRA-like population.

Conclusions: These findings indicate that the exercise intervention was not associated with broad changes in circulating immune composition in pediatric cancer patients but may instead have been associated with changes in the relative proportions of specific immune populations and/or their distribution within the circulation. Exploratory analyses identified three exercise-associated immune signatures that warrant confirmation in larger, adequately powered studies.

KEYWORDS

childhood cancer, FORTEe trial, immune function, metaclusters, spectral flow cytometry

1 Introduction

Exercise interventions have gained increasing attention as supportive strategies in pediatric oncology, with growing evidence demonstrating beneficial effects on key clinical outcomes, including cardiorespiratory fitness, muscle strength, and physical function (1). However, despite these advances, the biological mechanisms underlying exercise-induced adaptations in children with cancer remain incompletely understood, particularly at the level of immune system regulation (1, 2).

The immune system plays a central role in childhood cancer progression, treatment response, and recovery, and is profoundly affected and in some cases directly targeted, by anticancer therapies (3–8). In pediatric patients with solid tumors, treatment- and tumor-related immune perturbations include lymphopenia, impaired cytotoxic function, chronic low-grade inflammation, and dysregulated antigen presentation (5, 9–11). These alterations may not only increase susceptibility to infections but also compromise tissue repair, functional recovery, and potentially antitumor immune surveillance (5, 12–15), underscoring the fundamental role of immune competence in host defense, tissue homeostasis, and tumor control. Despite the clinical relevance of these processes, the impact of supportive interventions such as exercise on immune dynamics in this population remains poorly characterized.

In adult oncology, exercise has been associated with improvements in several components of antitumor immunity, including the mobilization and redistribution of cytotoxic lymphocytes, increased natural killer (NK) cell activity, and attenuation of chronic inflammation (16, 17). However, whether these effects translate to pediatric populations remains unclear. Childhood cancers differ substantially from adult malignancies in terms of tumor biology, treatment intensity, and developmental immune status (18), which may critically influence the nature and magnitude of exercise-induced immune responses.

To date, studies in pediatric exercise oncology have primarily focused on feasibility, safety, and functional outcomes, with relatively limited exploration of immunological endpoints (19–21). Moreover, those studies assessing immune responses have largely relied on conventional approaches, typically restricted to global leukocyte counts or a limited set of markers (1, 19–21). Such approaches may not adequately capture the complexity and specificity of exercise-induced immune adaptations.

Large multicenter initiatives such as the FORTEe ("Get strong to fight childhood cancer") randomized controlled trial (RCT) (ClinicalTrials.gov ID NCT05289739) represent a major step forward in the field, providing robust clinical data on the implementation of structured exercise programs during anticancer treatment (22). However, the inherent clinical heterogeneity of these cohorts may limit the identification of tumor-type–specific and mechanistically relevant immune adaptations, particularly when analyzed using conventional methodologies. In this context, children with solid tumors constitute a biologically distinct subgroup characterized by specific tumor–immune interactions, treatment exposures, and systemic inflammatory profiles (5, 23, 24). A more focused analysis within this population may therefore provide critical insights into how exercise interacts with the immune system in a clinically meaningful context.

Effective antitumor immunity depends on coordinated interactions among multiple innate and adaptive immune-cell populations, including antigen-presenting and cytotoxic effector cells. Understanding how exercise influences these interactions is particularly relevant in pediatric oncology, where both the disease and its treatment can profoundly affect immune function, with potential implications for treatment response, recovery, and long-term outcomes (3, 6).

In this ancillary sub-study conducted within the framework of the FORTEe RCT, we address these knowledge gaps by using high-dimensional spectral flow cytometry. This approach enables a

comprehensive, high-resolution characterization of circulating immune cell populations, moving beyond global descriptors to identify exercise-associated changes in specific cell subsets.

Therefore, the aim of this study was to evaluate the effects of an 8-10–week exercise intervention on immune system-related outcomes in pediatric patients with solid tumors, with a particular focus on exploring exercise-associated alterations in specific immune-cell populations using high-dimensional profiling.

2 Materials and methods

2.1 Participants and study design

The present ancillary study included only FORTEe participants diagnosed with solid tumors and recruited across three institutions.

The FORTEe RCT was performed according to recent CONSORT-C guidelines (25). Between 01.04.2022 and 31.10.2024, participants were recruited at ten centers in Europe. The FORTEe study protocol and associated documents were approved by the Ethics Committee of the Rhineland-Palatinate Chamber of Physicians, the consortium's lead ethics committee, on 04.08.2021 (application number 2021–15904), followed by approvals from local ethics committees and regulatory authorities at each recruitment center. All procedures were conducted in accordance with the 1964 Declaration of Helsinki and its later amendments. Written informed consent was obtained from all participants (or their legal guardians for minors), with documented assent collected from children aged ≥6 years where possible. The FORTEe trial was prospectively registered in the German Clinical Trials Register (DRKS00027978) on 28.01.2022 and on ClinicalTrials.gov (NCT05289739) on 21.03.2022. Details of the study design have been published previously (22).

Patients were eligible if they: 1) were diagnosed with cancer according to the International Classification of Childhood Cancer, Third Edition (ICCC-3); 2) were between 4 and 21 years of age; 3) were undergoing chemotherapy and/or radiotherapy; 4) were determined to be suitable by the treating team; 5) provided written informed consent (and documented assent, when appropriate); 6) had sufficient proficiency in the national language or English; 7) and were not in the terminal phase of the disease. In the parent trial, participants were randomly assigned to either an exercise intervention group or a control group receiving usual care (22). Randomization and allocation procedures are described in the primary FORTEe publication.

The sample analyzed in the present study represents a subsample of FORTEe participants with solid tumors only, recruited across three institutions: University Medical Center Mainz (UMC-Mainz, Germany), Hospital Infantil Universitario Niño Jesús (HIUNJ, Spain), and Fondazione IRCCS Istituto Nazionale dei Tumori (INT, Italy).

Assessments were conducted at two timepoints: before the start of the intervention period (T0, typically aligned with the initiation of a new treatment cycle) and immediately following completion of the intervention period (T1).

2.2 Exercise intervention

Participants allocated to the intervention group received a personalized, supervised multimodal exercise program as described in detail in the main FORTEe RCT protocol (22). The intervention lasted 8–10 weeks, depending on individual treatment scheduling. The program combined age-appropriate endurance, resistance, flexibility, coordination/balance, and gait-training modalities tailored to each participant's clinical status and physical capacity. The intervention was designed to achieve 3–5 supervised sessions per week whenever clinically feasible. Sessions typically lasted 45–60 minutes, were prescribed at moderate intensity whenever possible, and were individually adjusted according to the participant's clinical condition and treatment schedule.

Exercise intensity was classified as moderate-to-vigorous when at least two of three predefined criteria were met: (i) therapist-rated signs of exertion, including breathing rate and sweating; (ii) a rating of perceived exertion ≥12 on the Borg 6–20 scale; and (iii) for endurance exercise, a heart rate ≥65% of maximum heart rate, determined by cardiopulmonary exercise testing or estimated as 208 − 0.7 × age (in years), or, for resistance exercise, the predefined repetition-load criterion described in the FORTEe protocol (22).

For each session, total exercise duration and time spent in the different exercise modalities were documented. Attendance, cancelled or prematurely terminated sessions, and the underlying reasons were also prospectively recorded.

2.3 PBMC isolation and cryopreservation

Peripheral blood mononuclear cells (PBMCs) were isolated from whole blood collected in EDTA tubes using density gradient centrifugation. Whole blood was gently layered over Ficoll®-Paque Plus and centrifuged at 300 × g for 15 minutes at room temperature with the brake turned off.

Following centrifugation, plasma was carefully collected and stored at −80 °C. The PBMC layer was then harvested, washed with phosphate-buffered saline (PBS), and centrifuged at 120 × g for 10 minutes without brake. This washing step was repeated three times to remove residual platelets and density gradient medium.

Cells were counted using a hemocytometer and resuspended in a cold freezing medium consisting of 10% dimethyl sulfoxide in fetal bovine serum. Samples were initially stored at −80 °C for 48 hours in a controlled-rate freezing container (Mr. Frosty) and subsequently transferred to liquid nitrogen for long-term storage.

To monitor and minimize batch-related variability in spectral flow cytometry analyses, PBMCs isolated from buffy coats were processed, cryopreserved, and analyzed under identical conditions and served as reference samples across experimental runs.

2.4 Thawing and viability assessment

Cryopreserved PBMCs were rapidly thawed in a 37 °C water bath and washed twice with 10 mL PBS, followed by centrifugation at 120 × g for 5 minutes. Cells were resuspended in 1 mL PBS.

Cell viability was assessed using acridine orange/propidium iodide (AO/PI) staining (ViaStain AOPI Staining Solution).

Briefly, 10 µL of cell suspension was mixed 1:1 with AO/PI solution, incubated for 5 minutes at room temperature in the dark, and subsequently loaded onto a counting slide. Viability was quantified using an automated Cellometer K2 (Revvity, Waltham, MA).

Viability was defined as the proportion of live (green fluorescent) cells relative to total nucleated cells. Samples with viability >25% were included in downstream analyses. The distribution of post-thaw viability across study groups and time points is shown in Supplementary File 1. Sequential gating counts and sample recovery information are provided in Supplementary Table S1.

Importantly, downstream flow cytometry analyses included stringent gating strategies to exclude debris, dead cells, and aggregates, ensuring that analyses were performed exclusively on viable singlet cells. In addition, multiple wash steps and filtration procedures were applied during sample preparation, further minimizing the impact of non-viable cells on immunophenotypic analyses.

2.5 Staining procedure

Cells were filtered using 70 µm Filcon strainers (BD Biosciences, Franklin Lakes, NJ) and split into three separate tubes for: (i) unstained control acquisition, (ii) immunophenotyping panel staining, and (iii) NK phenotype panel staining.

To prevent non-specific binding, Fc receptors were blocked by incubating cells for 15 minutes at room temperature in a blocking solution containing PBS supplemented with 1 mM EDTA, 1% FBS, and True-Stain Monocyte Blocker™.

Cells were then incubated with LIVE/DEAD™ Fixable Blue Dead Cell stain (UV excitation) for 15 minutes, washed with buffer, and resuspended in PBS containing EDTA, bovine serum albumin, and blocking agent.

For the immunophenotyping panel, antibodies were added sequentially as follows: C-C chemokine receptor type 7 (CCR7) for 10 minutes, followed by CCR6, CCR5, C-X-C motif chemokine receptor 5 (CXCR5), and CXCR3 for an additional 10 minutes. Cells were then incubated with T-cell receptor gamma delta (TCRγδ) antibody for 10 minutes, after which the remaining antibodies (Supplementary File 2) were added and incubated for 25 minutes.

For the NK phenotype panel, cells were incubated for 25 minutes at room temperature with the antibody cocktail detailed in Supplementary File 3.

All staining steps were performed in the dark at room temperature. Unstained samples were subjected to identical conditions except for antibody addition and were used solely for spectral unmixing and quality-control procedures, without being included in downstream high-dimensional clustering analyses.

After staining, cells were washed, resuspended in 200 µL PBS, and stored at 4 °C protected from light until acquisition.

2.6 Spectral flow cytometry

Data acquisition was performed using a Cytek Aurora spectral flow cytometer (Cytek Biosciences, Fremont, CA) following the manufacturer's recommendations. Daily quality control and calibration were conducted using reference beads to ensure instrument stability and spectral consistency.

Single-stained controls and unstained samples were acquired for spectral unmixing. Samples with visible aggregation were filtered prior to acquisition and analyzed at medium flow rates to minimize coincident events.

Fluorescence signals were collected across the full emission spectrum and unmixed using SpectroFlo software (Cytek Biosciences). Data preprocessing included selection of stable acquisition regions and exclusion of debris, doublets, and dead cells using sequential gating strategies.

Data were exported in Flow Cytometry Standard (FCS) and analyzed using OMIQ cloud-based software (OMIQ Inc., Santa Clara, CA). To control for batch effects, a reference sample stained with each panel was acquired across different experimental runs.

2.7 High-dimensional preprocessing

Data preprocessing and initial analyses were conducted using SpectroFlo (Cytek Biosciences) and GraphPad Prism (v8). High-dimensional analyses were performed on spectral flow cytometry datasets following spectral unmixing.

Live, gated cell populations were uploaded into OMIQ and further processed using PeacoQC (Ghent University/VIB, Ghent, Belgium) to remove technical artifacts and low-quality events. Unsupervised clustering was performed using Flow Self-Organizing Map (FlowSOM) (Ghent University/VIB, Ghent, Belgium) on the immunophenotyping panel. For the NK panel, clustering analysis was performed within the $CD45^+$ $CD56^+$ $CD3^-$ gated population (see Supplementary File 4). Metaclusters — defined as groups of phenotypically similar cell clusters, i.e., "clusters of clusters" — were generated using consensus clustering approaches, and Z-score–normalized heatmaps were constructed to visualize relative marker expression (median fluorescence intensity, MFI) across clusters. EmbedSOM visualizations were generated from these unsupervised high-dimensional analyses and should not be interpreted as conventional manual flow-cytometry gating plots.

2.8 Statistical analysis

Participants' baseline characteristics were summarized using descriptive statistics, with continuous variables presented as mean ± standard deviation and categorical variables presented as absolute numbers and percentages. The effects of exercise intervention on immune parameters were evaluated using a two-way mixed ANOVA, with group (exercise vs. control) as the between-subject factor and time (T0 vs. T1) as the within-subject factor. The group-by-time interaction was considered the primary effect of interest. Given the exploratory nature of this ancillary study and the large number of metaclusters evaluated, nominal p values are presented alongside p values adjusted for multiple comparisons using the Benjamini-Hochberg procedure to control the false discovery rate (FDR). Emphasis is placed on the FDR-adjusted results when interpreting evidence for differential exercise-associated changes.

3 Results

3.1 Main study characteristics

Twenty-nine participants had paired samples available and were therefore included in the present ancillary analysis, with 14 and 15 participants allocated in the exercise and control group, respectively. The flow diagram of study participants is shown in Figure 1 and their main demographic and clinical characteristics are summarized in Table 1. No significant between-group differences were observed at baseline (T_0), indicating appropriate comparability between the control and exercise groups prior to the intervention.

Participants in the exercise group completed on average a total of 19.5 ± 8.6 training sessions (or 1.7 ± 0.9 sessions per week) during the intervention period, corresponding to an attendance rate of 65.1 ± 27.8% of scheduled supervised sessions. Mean total training volume was 812 ± 477 minutes. The most frequent dominant exercise modalities were endurance (26%), resistance (43%), and coordination/balance training (18%). Reasons for missed or cancelled sessions included scheduling or logistical constraints (37%), medical or treatment-related issues (48%), and refusal by the participant or legal guardian (15%).

3.2 Exercise intervention does not alter the distribution of major circulating immune populations

The relative abundance of major immune populations was quantified in thawed PBMCs, based on surface-marker expression within viable $CD45^+$ leukocytes (Table 2). We found no group-by-time interactions (all $p > 0.1$) for any of the immune populations analyzed ($CD4^+$ T cells, $CD8^+$ T cells, B cells, NK cells, and monocytes). These findings suggest that the exercise intervention was not associated with detectable changes in the relative abundance of major circulating immune cell subsets.

3.3 Exercise intervention does not modify NK cell phenotype or metacluster distribution

To further examine the potential association between exercise on the NK cell compartment, unsupervised clustering analysis was performed using NK-associated markers, resulting in the identification of 10 NK cell metaclusters representing cytotoxic, activated, mature, and senescent phenotypes (Figure 2).

Event counts and relative frequencies for all NK-cell metaclusters are provided in Supplementary Table S2. The relative abundance of each NK cell metacluster remained unchanged over time in both control and exercise groups ($p > 0.05$, Figure 2A).

Phenotypic changes were further explored through Z-score–normalized heatmaps of MFI values for markers associated with cytotoxicity, activation, and inhibitory signaling, including CD56, CD57, CD16, NKp46, NKp30, NKG2D, CD69, KIR3DL1/3DS1, KIR2DL1, KIR2DL2/3, CD161, NKG2A, and SIGLEC7 (Figures 2B–E). No significant group-by-time interaction was found (all $p > 0.05$).

Collectively, these results indicate that the exercise intervention was not associated with detectable changes in NK cell distribution, differentiation status, activation profile, or receptor expression during the study period.

3.4 High-dimensional analysis identifies 20 immune metaclusters

To obtain a comprehensive view of the immune landscape, unsupervised clustering analysis was performed using spectral flow cytometry data. This approach identified 20 phenotypically distinct

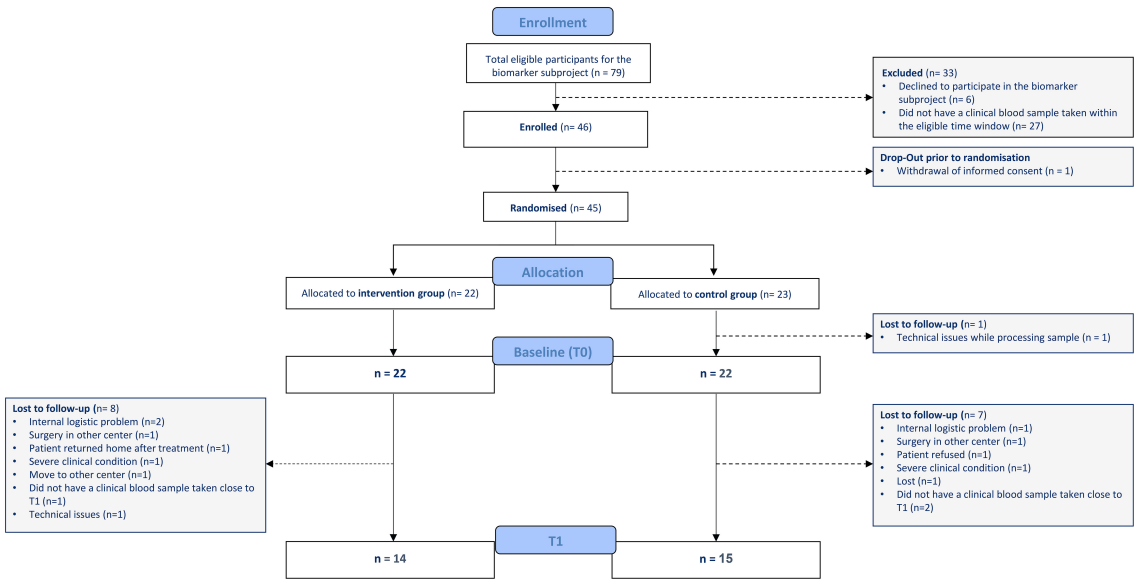


FIGURE 1
Flow diagram of study participants.

10.3389/fimmu.2026.1993392

TABLE 1 Main characteristics of study participants.

Main characteristics	Control group (n = 15)	Exercise group (n= 14)	P-value between-groups*
Sex, n (% male)	9 (60%)	6 (43%)	0.356
Age (years)	13.5 ± 3.2	12.9 ± 4.1	0.698
BMI	19.9 ± 3.9	20.0 ± 4.3	0.954
Lansky score at T0	85.5 ± 10.4	78.2 ± 21.8	0.335
Karnofsky score at T0	80.0 ± 8.2	70.0 ± 10.0	0.203
Diagnosis			
CNS tumors	3 (20%)	2 (14%)	1.000
Neuroblastoma	1 (7%)	3 (21%)	0.330
Renal tumors	1 (7%)	1 (7%)	1.000
Malignant bone tumors	7 (47%)	6 (43%)	0.837
Soft tissue sarcomas	3 (20%)	2 (14%)	1.000
Oncological disease status			
Initial cancer diagnosis	11 (73%)	12 (86%)	0.651
First relapse	4 (27%)	2 (14%)	0.651
Metastases present at initial diagnosis?			
Yes	3 (20%)	4 (29%)	0.682
Treatment group			
Combined chemo- and radiotherapy	7 (47%)	10 (71%)	0.176
Chemotherapy only	7 (47%)	4 (29%)	0.316
Radiotherapy only	0 (0%)	0 (0%)	1.000
Immune therapy	2 (13%)	3 (21%)	0.651
Tumor surgery	14 (93%)	13 (93%)	1.000
Hematopoietic stem cell transplantation	2 (13%)	2 (14%)	1.000
Hospital			
UMC-Mainz (Germany)	3 (43%)	4 (57%)	0.682
HIUNJ (Spain)	3 (50%)	3 (50%)	1.000
INT (Italy)	9 (56%)	7 (44%)	0.588

Data are presented as mean ± standard deviation or as n (%). Percentages may not total 100% due to rounding.
* Comparisons between groups were performed with an unpaired Students' t-test for data presented as mean ± standard deviation, or a χ^2 test (or a Fisher´s test when <80% of the cells had the expected frequency of n ≥ 5), for data presented as %). BMI, body mass index; CNS, central nervous system; HIUNJ, Hospital Infantil Universitario Niño Jesús; INT, Istituto Nazionale dei Tumori; T_0, pre-intervention.

metaclusters representing the major immune cell populations (Figure 3A).

These included: one monocyte population; two NK cell subsets; five $CD8^+$ T cell subsets; three $CD4^+$ T cell subsets; one double-negative ($CD4^-$ $CD8^-$) T cell population; three B cell populations; two myeloid-derived suppressor cell (MDSC) populations; and three dendritic cell (DC)-like populations.

The monocyte metacluster exhibited an intermediate/non-classical phenotype ($CD11b^+$ $CD57^+$ $CD127^+$ $CCR7^+$ $CD24^+$ $CD16^+$). NK cell metaclusters included highly cytotoxic $CD56^+$ $CD16^+$ effector populations and more mature $CD57^+$ subsets.

$CD8^+$ T cell populations comprised terminally differentiated effector memory cells (TEMRA)-like, regulatory-like subsets, and activated cytotoxic T cells expressing HLA-DR, PD-1, and PD-L1.

$CD4^+$ T-cell subsets included naïve, stem memory, and TEMRA-like populations. A separate double-negative ($CD4^-$ $CD8^-$) T-cell metacluster was also identified.

B-cell subsets were classified into immature, activated naïve, and late-differentiated IgG^+ populations.

In addition, DC-like subsets included conventional type 1 DCs (cDC1, i.e., $CD141^+$), cDC2 ($CD1c^+$), and a myeloid antigen-presenting population with DC-like features ($CD11b^+$ $CD14^+$ $CD16^+$ $CD141^+$ $CD95^+$), consistent with regulatory antigen-presenting phenotypes.

3.5 Three immune metaclusters showed nominally significant group-by-time interactions

Event counts and relative frequencies for all immune metaclusters are provided in Supplementary Table S3. Changes in metacluster abundance were evaluated to determine whether exercise assignment was associated with differential changes in specific immune cell subsets (Figure 3B). Two-way mixed ANOVA revealed significant group-by-time interactions for metaclusters 01 (MC-01; $p = 0.014$), 02 (MC-02, $p = 0.031$), and 04 (MC-04; $p = 0.030$), indicating differential temporal patterns between groups. The relative abundance of MC-01 (+11.3%) and to a much lesser degree of MC-02 (+0.9%) increased in controls but both populations decreased in the exercise group (−2.0% and −3.1%, respectively) whereas the MC-04 population decreased in controls (−4.4%) while increasing in the exercise group (+5.0%). However, statistical significance was lost after FDR-correction for multiple comparisons (Supplementary File 5).

MC-01 displayed a phenotype characterized by CD11b, CD11c, CD14, CD16, CD95, and CD141 expression, consistent with a myeloid antigen-presenting population with DC-like features (Figures 4A, B).

MC-02 population expressed CD19, CD20, CD45RA, and HLA-DR, consistent with mature B cells (Figures 4C, D).

MC-04 corresponded to a $CD8^+$ TEMRA-like population characterized by $CD8^+$ $CD45RA^{dim}$ $CD57^{dim}$ expression (Figures 4E, F). This population exhibited loss of co-stimulatory molecules CD27 and CD28 together with CD57 expression, consistent with an advanced differentiation state (Supplementary File 6). The additional expression of CD16 is compatible with features previously reported in highly differentiated cytotoxic $CD8^+$ T cell populations (26, 27).

Taken together, these exploratory findings suggest a possible association between exercise assignment and changes in the relative abundance of a $CD8^+$ TEMRA-like population, mature B cells and a myeloid antigen-presenting population with DC-like features, with no concomitant changes in the NK cell compartment. However, as these observations did not retain statistical significance after correction for multiple comparisons, they should be interpreted as hypothesis-generating findings. Hence, their functional relevance cannot be determined from the present study.

TABLE 2 Percentage distribution of main immune populations.

Cell subtype (%)	Control (T0)	Control (T1)	Exercise (T0)	Exercise (T1)	Group effect	Time effect	Group-by- time effect
$CD4^+$ cells	25.6 ± 14.6	29.8 ± 11.6	23.4 ± 13.5	17.5 ± 12.7	P = 0.021	P = 0.778	P = 0.764
$CD4^+$ $CD8^+$ cells	0.36 ± 0.36	0.19 ± 0.18	0.18 ± 0.19	0.22 ± 0.20	P = 0.206	P = 0.367	P = 0.188
$CD8^+$ cells	16.2 ± 6.3	11.1 ± 4.5	11.8 ± 5.7	14.9 ± 8.7	P = 0.113	P = 0.470	P = 0.195
B cells	7.8 ± 6.6	11.5 ± 12.1	10.3 ± 9.1	9.9 ± 10.7	P = 0.696	P = 0.078	P = 0.469
NK cells	12.0 ± 7.6	10.7 ± 5.7	7.9 ± 4.4	12.4 ± 6.7	P = 0.752	P = 0.417	P = 0.107
NK^{bright} cells	0.79 ± 1.11	1.56 ± 1.54	0.31 ± 0.33	1.19 ± 0.06	P = 0.063	P = 0.202	P = 0.759
Monocytes	5.1 ± 4.3	4.7 ± 2.9	4.5 ± 3.3	6.0 ± 6.2	P = 0.913	P = 0.887	P = 0.413

Relative abundance (%) of major circulating immune cell populations in control and exercise groups at baseline (T_0) and post-intervention (T_1). Data are presented as mean ± SD. Group, time, and group-by-time interaction effects were analyzed using two-way mixed ANOVA. Percentages of $CD4^-$ $CD8^-$ lymphocytes, other double-negative populations, dendritic cells, and other low-frequency cell subsets are not shown in this table.

4 Discussion

This study provides a high-resolution characterization of immune signatures associated with exercise in pediatric patients with solid tumors. Using spectral flow cytometry combined with unsupervised clustering, our results indicate that a structured exercise intervention was not associated with broad changes in the distribution of circulating immune cell populations. Instead, exploratory analyses identified nominal group-by-time interactions in three specific immune metaclusters. These observations support the possibility that exercise may be associated with selective modulation of discrete immune-cell subsets rather than global alterations in immune composition. Importantly, these exercise-associated immune signatures were only detectable through high-dimensional unsupervised analyses and would likely have remained unnoticed using conventional immune-cell quantification approaches. However, the group-by-time interactions observed for MC-01, MC-02, and MC-04 should be interpreted cautiously given the exploratory nature of the analyses and the relatively small sample size. In fact, statistical significance was lost after correction for multiple comparisons.

We observed no significant exercise-induced changes in the relative frequencies of major immune populations, including T cells, B cells, NK cells, and monocytes. These results align with previous studies in pediatric oncology, which have reported preservation of overall immune homeostasis following exercise interventions despite improvements in clinical and functional outcomes (2, 19–21). Similar observations have been reported in adult populations, where exercise training is associated with stable leukocyte distributions coupled with improved immune competence and systemic resilience (28, 29). Importantly, these findings provide no evidence that exercise adversely affected circulating immune-cell distributions. Moreover, despite the relatively low exercise exposure imposed by treatment-related constraints (1.7 ± 0.9 sessions/week on average), potential selective immune adaptations were still detected. Although exploratory, this observation suggests that clinically feasible exercise programs may still exert measurable immunomodulatory effects during active cancer treatment.

Our analysis of the NK cell compartment further supports this concept, as no significant changes were detected in NK cell metacluster distribution or phenotypic marker expression. Although NK cells are highly responsive to acute exercise stimuli, these responses are typically transient and driven by catecholamine-mediated β2-adrenergic signaling and hemodynamic forces (16, 17, 29, 30). Acute exercise preferentially mobilizes cytotoxic $CD56^{dim}$ NK cells into the circulation, followed by their redistribution to peripheral tissues, including tumor sites (30). The absence of detectable changes in the present study may be related to the timing of sample collection under resting conditions, together with the moderate intensity and frequency of the intervention. These findings highlight the importance of distinguishing between acute immune mobilization and longer-term exercise-associated immune changes when interpreting exercise immunology data.

In contrast to the stability observed in global immune parameters, our high-dimensional analysis identified nominal group-by-time differences in three immune metaclusters. Among these, the $CD8^+$ TEMRA-like population (MC-04) was of particular interest given its highly differentiated phenotype. This metacluster was characterized by CD45RA re-expression, loss of CD27 and CD28, and expression of CD57, features that have previously been associated with advanced T-cell differentiation (31–35). Although the biological significance of changes in this population remains uncertain, highly differentiated $CD8^+$ TEMRA-like cells have been implicated in immune surveillance and effector responses in a variety of clinical contexts (31–35). Accordingly, the observed pattern may warrant further investigation in larger studies specifically designed to assess exercise-associated immune adaptations. Notably, this $CD8^+$ TEMRA-like population increased in the exercise group while declining in controls. Although exploratory and not statistically significant after correction for multiple comparisons, this pattern may suggest relative preservation of a highly differentiated $CD8^+$ T-cell phenotype in participants assigned to exercise. However, functional competence was not assessed and therefore no conclusions can be drawn regarding the biological consequences of these changes. This observation may nevertheless be of interest in oncological settings, where T-cell dysfunction, exhaustion, and treatment-induced lymphodepletion are common features (36). Previous studies have proposed several mechanisms through which exercise may influence T-cell biology, including effects on cell trafficking, mitochondrial function, and cellular metabolism (37). However, whether such mechanisms contribute

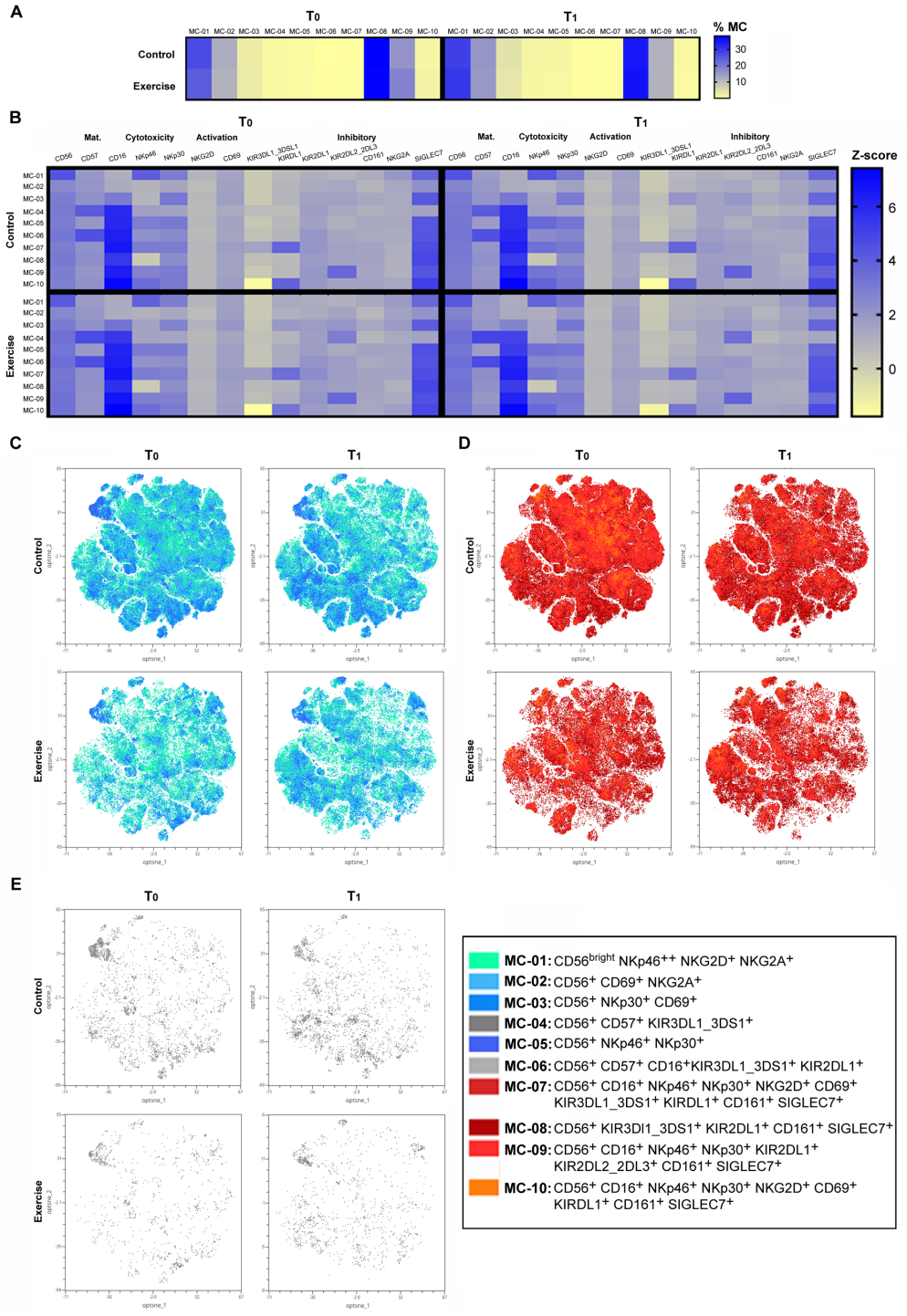


FIGURE 2
Unsupervised immunophenotypic characterization of circulating NK cell populations. Metacluster identifiers (MC-01 to MC-10) are shown to facilitate cross-referencing across figures, tables, and Supplementary Materials. **(A)** Relative abundance (%) of the 10 NK cell metaclusters identified by unsupervised clustering analysis in control and exercise groups at baseline (T_0) and post-intervention (T_1). Data are represented as a heatmap of the % abundance of each metacluster. **(B)** Heatmap showing Z-score–normalized median fluorescence intensity (MFI) values for NK cell–associated markers (CD56, CD57, CD16, NKp46, NKp30, NKG2D, CD69, KIR3DL1/3DS1, KIR2DL1, KIR2DL2/3, CD161, NKG2A, and SIGLEC7) across the 10 metaclusters. Color scaling represents relative marker expression after normalization. Mat.re, maturation-related markers. **(C–E)** Opt-SNE visualization of NK cell metaclusters grouped according to functional characteristics, including cytotoxic **(C)**, inhibitory **(D)**, and mature/senescent phenotypes **(E)**. Each metacluster is represented by a distinct color and annotated according to its phenotypic profile. These visualizations were generated from unsupervised high-dimensional analyses and should not be interpreted as conventional manual flow-cytometry gating plots. No significant group-by-time interaction was found by two-way mixed ANOVA for any NK-cell metacluster [$CD56^{bright}$ $NKp46^{++}$ $NKG2D^+$ $NKG2A^+$, p = 0.474; $CD56^+$ $CD69^+$ $NKG2A^+$, p = 0.640; $CD56^+$ $NKp30^+$ $CD69^+$, p = 0.374; $CD56^+$ $CD57^+$ $KIR3DL1_3DS1^+$, p = 0.569; $CD56^+$ $NKp46^+$ $NKp30^{++}$, p = 0.557; $CD56^+$ $CD57^+$ $CD16^+$ $KIR3DL1_3DS1^+$ $KIR2DL1^+$, p = 0.887; $CD56^+$ $CD16^+$ $NKp46^+$ $NKp30^+$ $NKG2D^+$ $CD69^+$ $KIR3DL1_3DS1^+$ $KIRDL1^+$ $CD161^+$ $SIGLEC7^+$, p = 0.288; $CD56^+$ $KIR3DL1_3DS1^+$ $KIR2DL1^+$ $CD161^+$ $SIGLEC7^+$, p = 0.437; $CD56^+$ $CD16^+$ $NKp46^+$ $NKp30^+$ $KIR2DL1^+$ $KIR2DL2_2DL3^+$ $CD161^+$ $SIGLEC7^+$, p = 0.606; $CD56^+$ $CD16^+$ $NKp46^+$ $NKp30^+$ $NKG2D^+$ $CD69^+$ $KIRDL1^+$ $CD161^+$ $SIGLEC7^+$, p = 0.564].

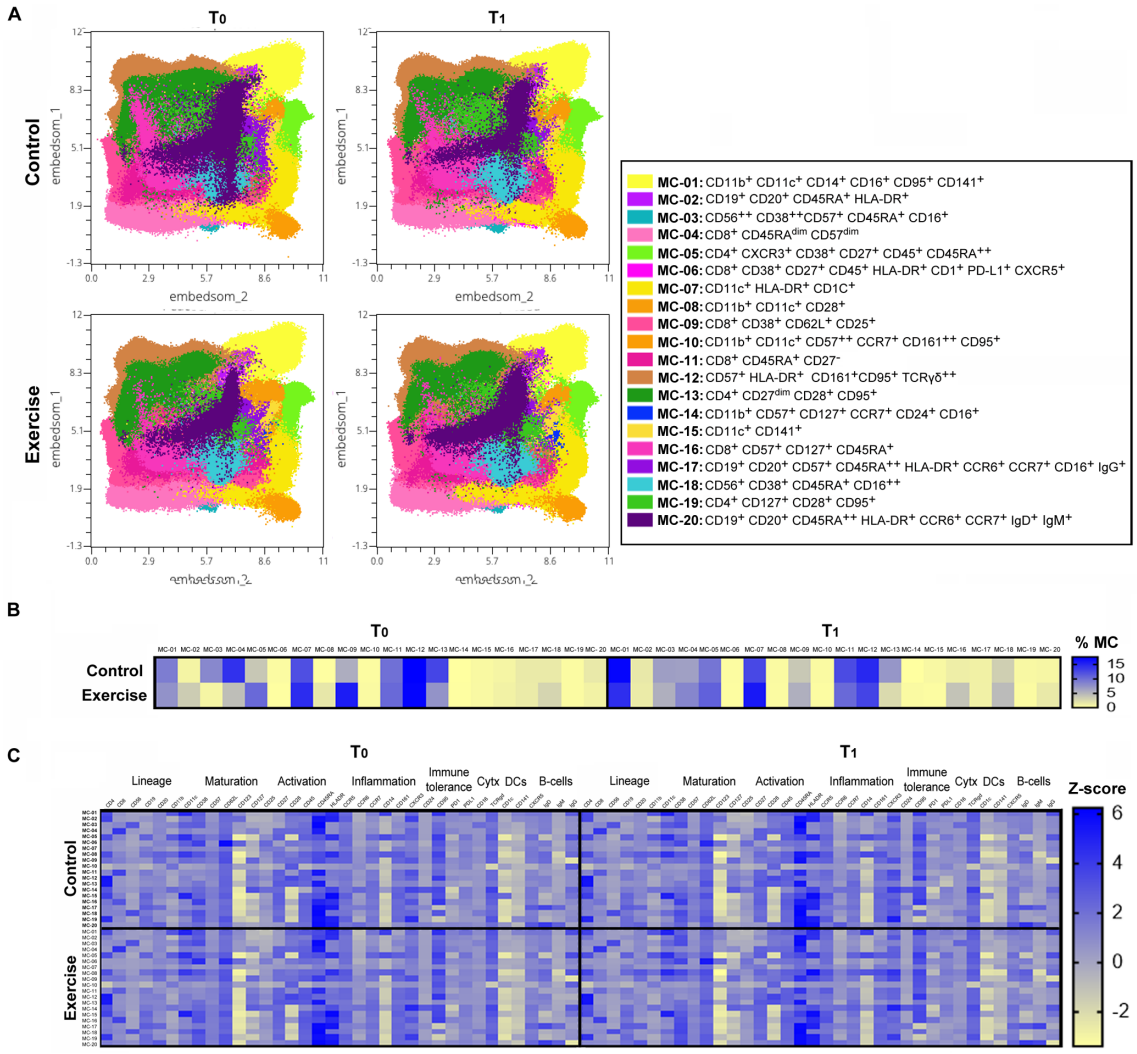


FIGURE 3
High-dimensional profiling of circulating immune populations. **(A)** EmbedSOM visualization of the 20 immune metaclusters identified by unsupervised clustering of spectral flow cytometry data. *Each metacluster (MC) is represented by a distinct color and identified by its corresponding metacluster number (MC-01 to MC-20). Colors: deep blue: monocytes, light blue: NK cells, pink: CD8 T cells, green: CD4 T-cells, purple: B-cells, yellow-orange: MDSCs and DCs). Metaclusters are annotated according to their phenotypic identity. **(B)** Relative abundance (%) of the 20 metaclusters in control and exercise groups at baseline (T_0) and post-intervention (T_1). Significant group-by-time interaction was found by Two-way Mixed ANOVA only for MC-01 (p=0.014), MC-02 (p=0.031) and MC-04 (p=0.030). However, neither remained statistically significant after correction for multiple testing (see Supplementary File 5). **(C)** Heatmap showing Z-score–normalized median fluorescence intensity (MFI) values for lineage, activation, differentiation, and regulatory markers (including CD4, CD8, CD56, CD19, CD20, CD11b, CD11c, CD38, CD57, CD62L, CD123, CD127, CD25, CD27, CD28, CD45, CD45RA, HLA-DR, CCR5, CCR6, CCR7, CD14, CD161, CXCR3, CD24, CD95, PD-1, PD-L1, CD16, TCRγδ, CD1c, CD141, CXCR5, IgD, IgM, and IgG). Color scaling indicates relative expression levels across metaclusters. Cytx: cytotoxicity; DCs: Dendritic cells.

to the patterns observed in the present study remains unknown and warrants further investigation.

Our observations are broadly consistent with previous evidence demonstrating preferential mobilization of differentiated cytotoxic lymphocytes in response to acute exercise, mediated by adrenergic-dependent mechanisms (16, 17, 29). In addition, exercise-induced redistribution of cytotoxic T cells has been linked to enhanced immune surveillance and improved antitumor responses (16, 30). Preclinical studies have shown that exercise training can increase tumor infiltration by cytotoxic lymphocytes and reduce tumor growth in an NK- and T cell–dependent manner (30). However, the present study was not designed to assess antitumor immune function, lymphocyte trafficking, or tumor infiltration. Accordingly, the observed changes should be considered hypothesis-generating rather than evidence of enhanced antitumor immunity.

Another metacluster showing a nominal group-by-time interaction (MC-01) displayed the phenotype of a myeloid antigen-presenting population with DC-like features. The increase in MC-01 frequency observed in the control group (+11.3%), contrasted with the mild decrease observed in the exercise group (–2.0%), may reflect differences in the distribution of circulating myeloid cells following the intervention. Monocytes and DCs contribute to inflammatory responses, antigen presentation, and immune surveillance, while their circulating abundance can be influenced by physiological stimuli, including exercise-induced leukocyte mobilization (38, 39). Notably, CD141 is a recognized marker of

10.3389/fimmu.2026.1993392

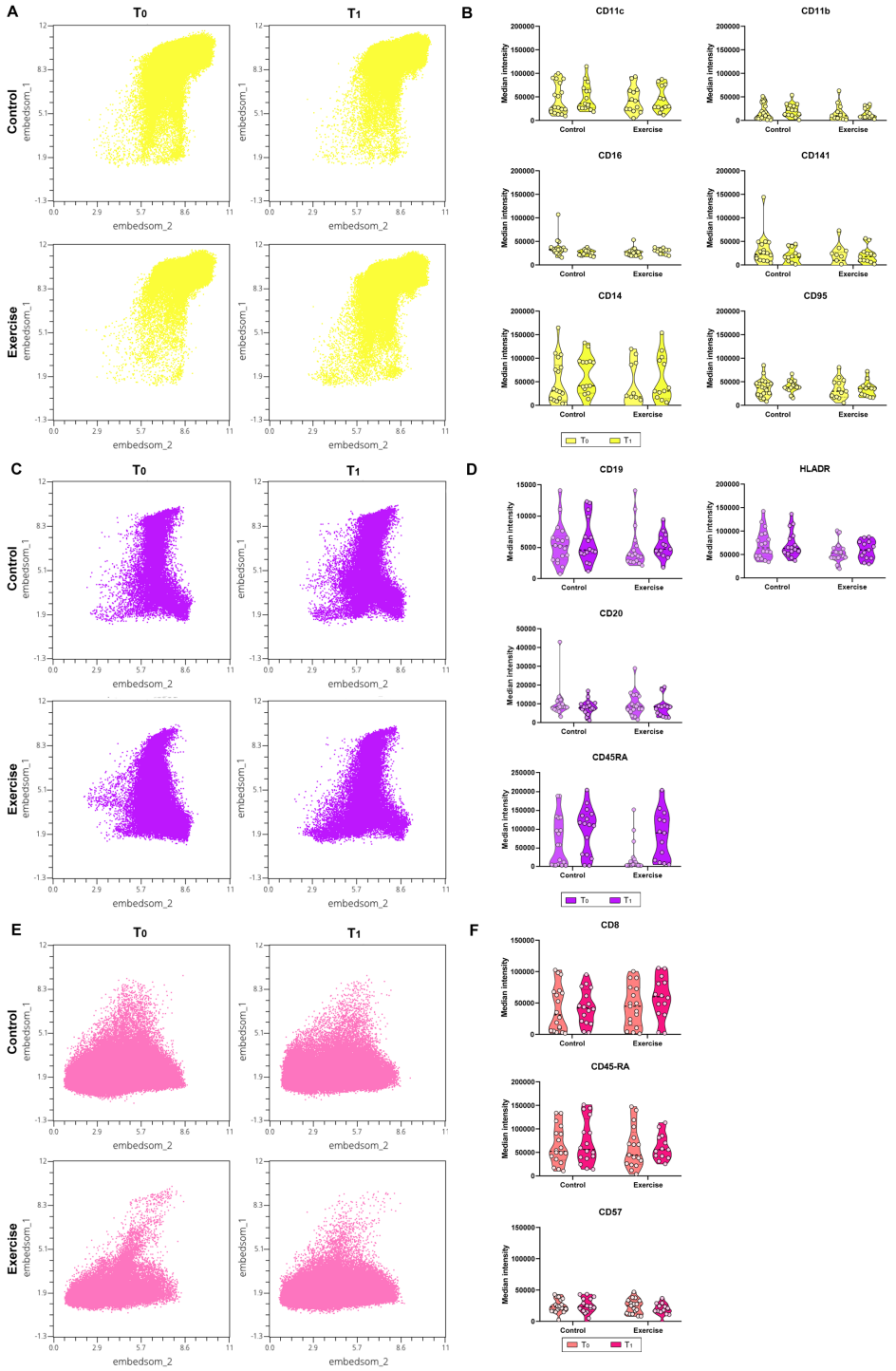


FIGURE 4
Exploratory exercise-associated immune signatures identified by high-dimensional analysis. **(A, C, E)** EmbedSOM representations of Metacluster 01 (MC-01), Metacluster 02 (MC-02) and Metacluster 04 (MC-04), respectively, in control and exercise groups at baseline (T_0) and after intervention (T_1). These visualizations were generated from unsupervised high-dimensional analyses of spectral flow-cytometry data and should not be interpreted as conventional manual flow-cytometry gating plots. **(B, D, F)** Median fluorescence intensity (MFI) plots of the principal phenotypic markers defining MC-01 **(B)**, MC-02 **(D)** and MC-04 **(F)**, illustrating their immunophenotypic profiles across groups and time points. MC-01 corresponds to a dendritic-like antigen-presenting population characterized by expression of CD11c, CD11b, CD14, CD16, and CD141. MC-02 is characterized by CD19, CD20, CD45RA and HLA-DR expression, compatible with a mature B cell population. MC-04 represents a highly differentiated $CD8^+$ TEMRA-like population characterized by CD45RAdim and CD57dim expression together with reduced CD27 and CD28 expression.

conventional type 1 DCs (cDC1) (40); however, its co-expression with CD14 and CD16 in MC-01 does not allow definitive assignment to a specific myeloid lineage or functional state. In the context of pediatric cancer, these changes may be relevant to understanding how exercise influences systemic immune composition; however, their functional and clinical implications remain uncertain. Given the absence of direct functional characterization, the observed decrease in MC-01 frequency should not necessarily be interpreted as reduced inflammation or improved immune function. Instead, it may indicate a differential redistribution of circulating myeloid populations, warranting further investigation using functional assays and more detailed immunophenotypic characterization.

Importantly, the concurrent pattern observed in this myeloid antigen-presenting population with DC-like features (MC-01) and the $CD8^+$ T_{EMRA}-like population (MC-04) may be of biological interest because these cell types participate in complementary aspects of immune responses (3, 6). However, the present study was not designed to assess interactions between immune-cell populations, antigen presentation, or T-cell priming. Consequently, the relationship between these observations remains speculative and should be interpreted cautiously. Nevertheless, future studies should investigate whether exercise-associated immune signatures involve coordinated changes across antigen-presenting and cytotoxic immune-cell compartments, particularly in the context of cancer. On the other hand, the observed decrease in circulating mature B-cells (MC-02) following the exercise intervention may reflect changes in B-cell trafficking or distribution rather than a direct reduction in immune competence. Although exercise can modulate circulating B-cell numbers, the physiological relevance of this phenomenon remains unclear (41).

A notable aspect of our findings is that these exploratory immune signatures were observed in the absence of detectable changes in major circulating immune populations. This pattern is consistent with the possibility that exercise may be associated with selective, rather than global, immune changes. However, given that the observed metacluster-level associations did not remain statistically significant after correction for multiple comparisons, this interpretation should be considered hypothesis-generating.

From a translational perspective, our findings raise hypotheses worthy of future investigation regarding potential interactions between exercise and cancer-related immune processes. However, because the present study was not designed to assess antitumor immunity, immunotherapy responsiveness, or clinical outcomes, any such implications remain speculative. The exploratory immune signatures identified herein may nevertheless provide a rationale for future studies examining whether exercise is associated with immune changes relevant to immunotherapy responses in pediatric cancer populations.

The present study also has several strengths. To our knowledge, this is the first study to comprehensively characterize exercise-associated immune signatures in children and adolescents with cancer using high-dimensional spectral flow cytometry and unsupervised clustering approaches within the context of a multicenter randomized controlled trial. The combination of a standardized exercise intervention, longitudinal sampling, and high-dimensional immune profiling enabled a detailed characterization of circulating immune-cell populations beyond conventional leukocyte-based analyses.

Several limitations should nevertheless be considered. First, the relatively low post-thaw cell viability observed in some samples may have introduced bias, as more fragile immune populations could have been preferentially affected by cryopreservation and processing procedures (42). However, stringent quality-control procedures, including exclusion of debris, dead cells, and doublets, ensured that all analyses were restricted to viable singlet cells. Second, all analyses were based on relative frequencies within PBMC-derived populations, and absolute immune-cell counts were not available. Therefore, changes in relative abundance should not be interpreted as changes in absolute cell numbers. Third, information regarding viral infections, viral reactivation, vaccination status, corticosteroid exposure, G-CSF administration, transfusions, surgery, and other potentially immune-modifying clinical factors was not consistently available across participants and study sites. Consequently, residual confounding related to concomitant treatments, timing of treatment exposure, prior antigen exposure, or other clinical events cannot be excluded. Accordingly, the observed changes in the proportion of highly differentiated immune cell populations should not be attributed solely to the exercise intervention.

Additional limitations include the relatively small sample size and the clinical heterogeneity inherent to pediatric solid tumors, which limited statistical power, precluded meaningful subgroup analyses, and may have contributed to the loss of statistical significance following correction for multiple comparisons. Accordingly, the observed associations should be considered exploratory and require independent validation in larger cohorts. Furthermore, because of ethical constraints regarding blood collection in pediatric oncology populations, our analyses were limited to immune phenotyping and did not include functional assessments such as cytotoxicity assays, cytokine production, antigen presentation, or antigen-specific immune responses. Therefore, the biological significance of the identified immune signatures remains uncertain. Future studies integrating functional assays, multi-omic approaches, longitudinal sampling, and detailed characterization of exercise dose, adherence, and physical-function responses will be essential to determine whether exercise-associated immune signatures translate into meaningful immunological or clinical adaptations.

In conclusion, this study indicates that a structured exercise intervention in pediatric patients with solid tumors was not associated with broad changes in circulating immune cell composition. However, exploratory analyses identified three exercise-associated immune signatures represented by a $CD8^+$ T_{EMRA}-like population, a mature B cell population, and a myeloid antigen-presenting population with DC-like features. Although these findings did not remain statistically significant after correction for multiple comparisons, they provide preliminary insight into potential immune pathways that may be influenced by exercise during cancer treatment. Accordingly, the present results should be considered exploratory and hypothesis-generating and require independent validation in larger cohorts. Future studies should determine whether modality-specific exercise prescriptions (e.g., aerobic, resistance, or combined training) elicit distinct immune

adaptations and differentially influence circulating immune-cell populations in pediatric oncology populations.

Data availability statement

The raw data supporting the conclusions of this article will be made available by the authors, without undue reservation.

Ethics statement

The FORTEe study was approved by the Ethics Committee of the Rhineland-Palatinate Chamber of Physicians. The FORTEe consortium's lead ethics committee, on 04.08.2021 (application number 2021 -15904), followed by approvals from local ethics committees and regulatory authorities at each recruitment center. The study was conducted in accordance with the local legislation and institutional requirements. Written informed consent for participation in this study was obtained from all participants (or their legal guardians for minors), with documented assent collected from children aged 6 years and above where possible.

Author contributions

NY: Conceptualization, Data curation, Formal analysis, Investigation, Methodology, Writing – original draft, Writing – review & editing. GS: Investigation, Writing – original draft, Writing – review & editing. RY-P: Investigation, Writing – review & editing, Writing – original draft. MK: Investigation, Writing – original draft, Writing – review & editing. JW: Investigation, Writing – original draft, Writing – review & editing. CF-L: Conceptualization, Data curation, Formal analysis, Funding acquisition, Investigation, Resources, Supervision, Writing – original draft, Writing – review & editing. JF: Writing – original draft, Writing – review & editing, Investigation. WZ: Investigation, Writing – review & editing, Writing – original draft. AL: Conceptualization, Investigation, Resources, Supervision, Writing – original draft, Writing – review & editing. PG: Investigation, Writing – review & editing, Writing – original draft. MC: Investigation, Writing – review & editing, Writing – original draft. FS: Investigation, Writing – review & editing, Writing – original draft. NL: Investigation, Writing – original draft, Writing – review & editing. EG-R: Investigation, Writing – review & editing, Writing – original draft. ED: Investigation, Writing – original draft, Writing – review & editing. MN: Conceptualization, Data curation, Formal analysis, Investigation, Project administration, Writing – review & editing, Writing – original draft. LW: Data curation, Formal analysis, Investigation, Writing – original draft, Writing – review & editing. AP-F: Investigation, Writing – review & editing, Data curation, Formal analysis, Writing – original draft. CP: Investigation, Writing – original draft, Writing – review & editing. ER: Investigation, Writing – review & editing, Writing – original draft.

Funding

The author(s) declared that financial support was received for this work and/or its publication. This project has received funding from the European Union's Horizon 2020 research and innovation program under grant agreement No. 945153. This publication reflects only the authors' views and the European Union is not liable for any use that may be made of the information contained therein. Research by C.F.L. is funded by Instituto de Salud Carlos III (ISCIII) and co-funded by the European Union through project nos. PI20/00645, PI23/00396 and FORT23/00023, and by the MCIN/AEI/10.13039/501100011033 and «Next Generation EU»/PRTR (project no. CNS2023-149 144144). Research by A.L. and C.F.-L. is funded by the Wereld Kanker Onderzoek Fonds, as part of the World Cancer Research Fund International grant programme (grant no. IIG_FULL_2021_007). A.P.F. was supported by PERC Systems Biology Fund.

Conflict of interest

The author(s) declared that this work was conducted in the absence of any commercial or financial relationships that could be construed as a potential conflict of interest.

Generative AI statement

The author(s) declared that generative AI was not used in the creation of this manuscript.

Any alternative text (alt text) provided alongside figures in this article has been generated by Frontiers with the support of artificial intelligence and reasonable efforts have been made to ensure accuracy, including review by the authors wherever possible. If you identify any issues, please contact us.

Publisher's note

All claims expressed in this article are solely those of the authors and do not necessarily represent those of their affiliated organizations, or those of the publisher, the editors and the reviewers. Any product that may be evaluated in this article, or claim that may be made by its manufacturer, is not guaranteed or endorsed by the publisher.

Supplementary material

The Supplementary Material for this article can be found online at: https://www.frontiersin.org/articles/10.3389/fimmu.2026.1993392/full#supplementary-material

References

1. Fridh MK, Kesting S, Neu MA, Valenzuela PL, Wogksch M, Culos-Reed SN, et al. Initial exercise guidance for children and adolescents during and beyond cancer treatment: ACSM expert consensus statement. *Med Sci Sports Exerc*. (2026) 58:1615–28. doi: 10.1249/MSS.0000000000003958

2. Beller R, Bennstein SB, Götte M. Effects of exercise interventions on immune function in children and adolescents with cancer and HSCT recipients - a systematic review. *Front Immunol*. (2021) 12:746171. doi: 10.3389/fimmu.2021.746171

3. Pathania AS. Immune microenvironment in childhood cancers: characteristics and therapeutic challenges. *Cancers*. (2024) 16:2201. doi: 10.3390/cancers16122201

4. Racacho KJ, Shiau YP, Villa R, Mahri S, Tang M, Lin TY, et al. The tumor immune microenvironment: implications for cancer immunotherapy, treatment strategies, and monitoring approaches. *Front Immunol*. (2025) 16:1621812. doi: 10.3389/fimmu.2025.1621812

5. Chen Q, Zhao B, Tan Z, Hedberg G, Wang J, Gonzalez L, et al. Systems-level immunomonitoring in children with solid tumors to enable precision medicine. *Cell*. (2025) 188:1425–1440.e11. doi: 10.1016/j.cell.2024.12.014

6. Guilcher GMT, Rivard L, Huang JT, Wright NAM, Anderson L, Eissa H, et al. Immune function in childhood cancer survivors: a Children's Oncology Group review. *Lancet Child Adolesc Health*. (2021) 5:284–94. doi: 10.1016/S2352-4642(20)30312-6

7. Vonderhaar EP, Dwinell MB, Craig BT. Targeted immune activation in pediatric solid tumors: opportunities to complement local control approaches. *Front Immunol*. (2023) 14:1202169. doi: 10.3389/fimmu.2023.1202169

8. Holterhus M, Altvater B, Kailayangiri S, Rossig C. The cellular tumor immune microenvironment of childhood solid cancers: informing more effective immunotherapies. *Cancers*. (2022) 14:2177. doi: 10.3390/cancers14092177

9. Hutzen B, Ghonime M, Lee J, Mardis ER, Wang R, Lee DA, et al. Immunotherapeutic challenges for pediatric cancers. *Mol Ther Oncolytics*. (2019) 15:38–48. doi: 10.1016/j.omto.2019.08.005

10. Ménétrier-Caux C, Ray-Coquard I, Blay JY, Caux C. Lymphopenia in cancer patients and its effects on response to immunotherapy: an opportunity for combination with cytokines? *J Immunother Cancer*. (2019) 7:85. doi: 10.1186/s40425-019-0549-5

11. Perl A, Morel L. Expanding scope of TEMRA in autoimmunity. *EBioMedicine*. (2023) 90:104520. doi: 10.1016/j.ebiom.2023.104520

12. Bergsma FJ, Koster J, Baalman B, Mussai F, Caron HN, Molenaar JJ, et al. The immune landscape of pediatric (extra)cranial solid tumors: a systematic review and integration of immunohistochemistry and single-cell RNA sequencing data. *Eur J Cancer*. (2025) 228:115708. doi: 10.1016/j.ejca.2025.115708

13. Elçioğlu ZC, Errington L, Metes B, Sendama W, Powell J, Simpson AJ, et al. Pooled prevalence of lymphopenia in all-cause hospitalisations and association with infection: a systematic review and meta-analysis. *BMC Infect Dis*. (2023) 23:848. doi: 10.1186/s12879-023-08845-1

14. Jakovija A, Chtanova T. Skin immunity in wound healing and cancer. *Front Immunol*. (2023) 14:1060258. doi: 10.3389/fimmu.2023.1060258

15. Guerrouahen BS, Maccalli C, Cugno C, Rutella S, Akporiaye ET. Reverting immune suppression to enhance cancer immunotherapy. *Front Oncol*. (2019) 9:1554. doi: 10.3389/fonc.2019.01554

16. Fiuza-Luces C, Valenzuela PL, Gálvez BG, Ramírez M, López-Soto A, Simpson RJ, et al. The effect of physical exercise on anticancer immunity. *Nat Rev Immunol*. (2024) 24:282–93. doi: 10.1038/s41577-023-00943-0

17. Campbell JP, Turner JE. Debunking the myth of exercise-induced immune suppression: redefining the impact of exercise on immunological health across the lifespan. *Front Immunol*. (2018) 9:648. doi: 10.3389/fimmu.2018.00648

18. Chen X, Yang W, Roberts CWM, Zhang J. Developmental origins shape the paediatric cancer genome. *Nat Rev Cancer*. (2024) 24:382–98. doi: 10.1038/s41568-024-00684-9.

19. Fiuza-Luces C, Padilla JR, Valentín J, Santana-Sosa E, Santos-Lozano A, Sanchis-Gomar F, et al. Effects of exercise on the immune function of pediatric patients with solid tumors: insights from the PAPEC randomized trial. *Am J Phys Med Rehabil*. (2017) 96:831–7. doi: 10.1097/PHM.0000000000000757

20. Chamorro-Viña C, Valentín J, Fernández L, González-Vicent M, Pérez-Ruiz M, Lucía A, et al. Influence of a moderate-intensity exercise program on early NK cell immune recovery in pediatric patients after reduced-intensity hematopoietic stem cell transplantation. *Integr Cancer Ther*. (2017) 16:464–72. doi: 10.1177/1534735416679515

21. Senn-Malashonak A, Wallek S, Schmidt K, Rosenhagen A, Vogt L, Bader P, et al. Psychophysical effects of an exercise therapy during pediatric stem cell transplantation: a randomized controlled trial. *Bone Marrow Transplant*. (2019) 54:1827–35. doi: 10.1038/s41409-019-0535-z

22. Neu MA, Dreismickenbecker E, Lanfranconi F, Stössel S, Balduzzi A, Wright P, et al. Get strong to fight childhood cancer - an exercise intervention for children and adolescents undergoing anti-cancer treatment (FORTEe): rationale and design of a randomized controlled exercise trial. *BMC Cancer*. (2025) 25:1275. doi: 10.1186/s12885-025-14489-y

23. Belgiovine C, Mebelli K, Raffaele A, De Cicco M, Rotella J, Pedrazzoli P, et al. Pediatric solid cancers: dissecting the tumor microenvironment to improve the results of clinical immunotherapy. *Int J Mol Sci*. (2024) 25:3225. doi: 10.3390/ijms25063225

24. Sherif S, Roelands J, Mifsud W, Ahmed EI, Raynaud CM, Rinchai D, et al. The immune landscape of solid pediatric tumors. *J Exp Clin Cancer Res CR*. (2022) 41:199. doi: 10.1186/s13046-022-02397-z

25. Baba A, Smith M, Potter BK, Chan AW, Moher D, Toulany A, et al. CONSORT-Children and Adolescents (CONSORT-C) 2026 extension statement: enhancing the reporting and impact of paediatric randomised trials. *BMJ*. (2026) 392:e085061. doi: 10.1136/bmj-2025-085061

26. De Pasquale C, Drommi F, Calabrò A, Botta C, Sidoti Migliore G, Carrega P, et al. BNT162b2 COVID-19 vaccination elicits the expansion of CD16+CD8+ T cells endowed with natural killer cell features. *J Allergy Clin Immunol*. (2025) 155:1981–92. doi: 10.1016/j.jaci.2025.01.024

27. Wang Q, Chen S, Guo Z, Xia S, Zhang M. NK-like CD8 T cell: one potential evolutionary continuum between adaptive memory and innate immunity. *Clin Exp Immunol*. (2024) 217:136–50. doi: 10.1093/cei/uxae038

28. Walsh NP, Gleeson M, Shephard RJ, Gleeson M, Woods JA, Bishop NC, et al. Position statement. Part one: immune function and exercise. *Exerc Immunol Rev*. (2011) 17:6–63

29. Simpson RJ, Kunz H, Agha N, Graff R. Exercise and the regulation of immune functions. *Prog Mol Biol Transl Sci*. (2015) 135:355–80. doi: 10.1016/bs.pmbts.2015.08.001

30. Pedersen L, Idorn M, Olofsson GH, Lauenborg B, Nookaew I, Hansen RH, et al. Voluntary running suppresses tumor growth through epinephrine- and IL-6-dependent NK cell mobilization and redistribution. *Cell Metab*. (2016) 23:554–62. doi: 10.1016/j.cmet.2016.01.011

31. Türk L, Filippov I, Arnold C, Zaugg J, Tserel L, Kisand K, et al. Cytotoxic CD8+ Temra cells show loss of chromatin accessibility at genes associated with T cell activation. *Front Immunol*. (2024) 15:1285798. doi: 10.3389/fimmu.2024.1285798

32. Appay V, Douek DC, Price DA. CD8+ T cell efficacy in vaccination and disease. *Nat Med*. (2008) 14:623–8. doi: 10.1038/nm.f.1774

33. Geginat J, Lanzavecchia A, Sallusto F. Proliferation and differentiation potential of human CD8+ memory T-cell subsets in response to antigen or homeostatic cytokines. *Blood*. (2003) 101:4260–6. doi: 10.1182/blood-2002-11-3577

34. Rodriguez IJ, Lalinde Ruiz N, Llano León M, Martínez Enríquez L, Montilla Velásquez MDP, Ortiz Aguirre JP, et al. Immunosenescence study of T cells: a systematic review. *Front Immunol*. (2020) 11:604591. doi: 10.3389/fimmu.2020.604591

35. Kasamatsu T. Implications of senescent T cells for cancer immunotherapy. *Cancers*. (2023) 15:5835. doi: 10.3390/cancers15245835

36. Wherry EJ, Kurachi M. Molecular and cellular insights into T cell exhaustion. *Nat Rev Immunol*. (2015) 15:486–99. doi: 10.1038/nri3862

37. Simpson RJ, Boßlau TK, Weyh C, Niemiro GM, Batatinha H, Smith KA, et al. Exercise and adrenergic regulation of immunity. *Brain Behav Immun*. (2021) 97:303–18. doi: 10.1016/j.bbi.2021.07.010

38. Simpson RJ, Bigley AB, Agha N, Hanley PJ, Bollard CM. Mobilizing immune cells with exercise for cancer immunotherapy. *Exerc Sport Sci Rev*. (2017) 45:163–72. doi: 10.1249/JES.0000000000000114

39. Khosravi N, Stoner L, Farajivafa V, Hanson ED. Exercise training, circulating cytokine levels and immune function in cancer survivors: a meta-analysis. *Brain Behav Immun*. (2019) 81:92–104. doi: 10.1016/j.bbi.2019.08.187

40. Jongbloed SL, Kassianos AJ, McDonald KJ, Clark GJ, Ju X, Angel CE, et al. Human CD141+ (BDCA-3)+ dendritic cells (DCs) represent a unique myeloid DC subset that cross- presents necrotic cell antigens. *J Exp Med*. (2010) 207:1247–60. doi: 10.1084/jem.20092140

41. Walzik D, Belen S, Wilisch K, Kupjetz M, Kirschke S, Esser T, et al. Impact of exercise on markers of B cell-related immunity: a systematic review. *J Sport Health Sci*. (2024) 13:339–52. doi: 10.1016/j.jshs.2023.10.002

42. Weinberg A, Song LY, Wilkening C, Sevin A, Blais B, Louzao R, et al. Optimization and limitations of use of cryopreserved peripheral blood mononuclear cells for functional and phenotypic T-cell characterization. *Clin Vaccine Immunol CVI*. (2009) 16:1176–86. doi: 10.1128/CVI.00342-08